Marine and Petroleum Geology 96 (2018) 154–165

Contents lists available at ScienceDirect

Marine and Petroleum Geology

journal homepage: www.elsevier.com/locate/marpetgeo

Research paper

# A preliminary study of the present-day in-situ stress state in the Ahe tight gas reservoir, Dibei Gasfield, Kuqa Depression

Wei Ju[a,b,*], Ke Wang[c]

[a] Key Laboratory of Coalbed Methane Resources and Reservoir Formation Process, Ministry of Education, China University of Mining and Technology, Xuzhou 221008, China
[b] School of Resources and Geosciences, China University of Mining and Technology, Xuzhou 221116, China
[c] PetroChina Hangzhou Research Institute of Geology, Hangzhou 310023, China

ARTICLE INFO

*Keywords:*
In-situ stress state
Dibei gasfield
Ahe formation
Tight gas
Borehole stability
Kuqa depression

ABSTRACT

Knowledge of the present-day in-situ stress state has significant applications in the exploration and development of tight gas reservoirs. The Ahe Formation is an important tight gas reservoir in the Dibei Gasfield of Kuqa Depression. However, prior to this study, little attention has been paid to the present-day in-situ stress field within the formation. In the present study, the in-situ stress orientation and magnitudes were investigated based on well log calculations and geomechanical modeling. The horizontal maximum principal stress ($S_{Hmax}$) orientation was determined from interpretations of drilling-induced tensile fractures (DITFs) and borehole breakouts in imaging logs, which showed variations between NNW-SSE-trending and NNE-SSW-trending in the Dibei Gasfield. The in-situ stress magnitudes were calculated in four wells based on well logs, the results indicated a normal faulting stress regime within the Ahe tight gas reservoir. Numerical simulation of the present-day in-situ stresses showed that the magnitudes of vertical stress ($S_v$), $S_{Hmax}$ and horizontal minimum principal stress ($S_{hmin}$) were −105.5 MPa ~ -191.0 MPa, −88.9 MPa ~ -142.9 MPa, and −79.1 MPa ~ -127.7 MPa within the Ahe Formation, respectively. In addition, considering the present-day in-situ stress state in the Ahe Formation of Dibei Gasfield, natural fractures in directions parallel/sub-parallel to the $S_{Hmax}$ orientation with high fracture angles showed great contributions to subsurface fluid flow. Borehole instability may become a potentially significant problem when drilling vertical wells and horizontal wells deviated toward the $S_{Hmax}$ orientation in the Ahe tight gas reservoir of Dibei Gasfield.

## 1. Introduction

In-situ stress refers to the internal stress within the Earth's crust, and is closely related to gravitational and tectonic stresses. The gravitational stress is mainly influenced by overlying rocks and can be estimated by the weight of overlying strata. On the contrary, tectonic stress is extremely complicated with an irregular spatial distribution and greatly influenced by tectonic movements during historical geologic periods (Bell, 1996; Kang et al., 2010; Ju et al., 2017a).

Assuming the vertical stress is one of the three principal stresses, the stress tensor is typically reduced to four components: the vertical stress ($S_v$) magnitude, horizontal maximum principal stress ($S_{Hmax}$) magnitude, horizontal minimum principal stress ($S_{hmin}$) magnitude, and the orientation of $S_{Hmax}$ (Bell, 1996; Zoback et al., 2003; Rajabi et al., 2016). Generally, these three principal stress magnitudes are unequal, and vary throughout a sedimentary basin both in burial depth and laterally. Three types of in-situ stress regime can be determined based on Anderson's categorization (Anderson, 1951), namely, i) normal faulting stress regime ($S_v > S_{Hmax} > S_{hmin}$), ii) strike-slip faulting stress regime ($S_{Hmax} > S_v > S_{hmin}$), and iii) reverse faulting stress regime ($S_{Hmax} > S_{hmin} > S_v$). Knowledge of in-situ stress state can help understanding the exploration and development of unconventional hydrocarbon reservoirs (Bell and Bachu, 2003; Kingdon et al., 2016; Nian et al., 2016; Ju et al., 2017a), borehole stability (Hillis and Williams, 1993; Moos et al., 2003; Gentzis, 2009; Tingay et al., 2009; Rajabi et al., 2016), reservoir management (Fuchs and Muller, 2001; Zoback et al., 2003; Binh et al., 2007), etc.

Tight gas, one type of unconventional resources, plays an important part in global natural gas production with the increasing development of natural gas extraction techniques (Higgs et al., 2007; Dai et al., 2012; Shi et al., 2018; Yue et al., 2018). The total tight gas production in United States is 1964.565 bcm (International Energy Agency, IEA,

* Corresponding author. Key Laboratory of Coalbed Methane Resources and Reservoir Formation Process, Ministry of Education, China University of Mining and Technology, Xuzhou 221008, China.
*E-mail address:* wju@cumt.edu.cn (W. Ju).

https://doi.org/10.1016/j.marpetgeo.2018.05.036
Received 26 February 2018; Received in revised form 20 April 2018; Accepted 31 May 2018
Available online 01 June 2018

**List of symbols**

| | |
|---|---|
| 3D | three-dimensional |
| AE | Acoustic Emission |
| $\alpha$ | Biot's coefficient |
| bcm | billion cubic meter |
| $\sigma$ | confining pressure |
| DITFs | drilling-induced tensile fractures |
| $E$ | static Young's modulus |
| $E_d$ | dynamic Young's modulus |
| EIA | Energy Information Administration |
| FE | finite element |
| $g$ | gravitational acceleration |
| $h$ | burial depth |
| $i$ | displacement along the $x$ axis |
| $j$ | displacement along the $y$ axis |
| $k$ | displacement along the $z$ axis |
| IEA | International Energy Agency |
| km | kilometer |
| m | meter |
| $m^3/d$ | cubic meter per day |
| $\mu$ | static Poisson's ratio |
| $\mu_d$ | dynamic Poisson's ratio |
| μm | micron |
| MPa | megapascal |
| $n$ | an exponent |
| NA | not applicable |
| $P_o$ | pore pressure |
| ρ | density |
| $Q$ | a function of pore pressure and confining pressure |
| $R$ | correlation coefficient |
| $r$ | the error between calculated and measured value |
| $S_h$ | hydrostatic pore pressure |
| $S_{Hmax}$ | horizontal maximum principal stress |
| $S_{hmin}$ | horizontal minimum principal stress |
| $S_v$ | vertical stress |
| $\Delta t$ | observed acoustic travel time |
| $\Delta t_{normal}$ | acoustic travel time from the normal compaction trend |
| $\upsilon_p$ | compressional wave velocity |
| $\upsilon_s$ | shear wave velocity |
| WSM | World Stress Map |
| $\varepsilon_{\max}$ | strain in the maximum stress direction |
| $\varepsilon_{\min}$ | strain in the minimum stress direction |
| $\varepsilon_{xx}$, $\varepsilon_{yy}$ and $\varepsilon_{zz}$ | the linear strain component |
| $\gamma_{xy}$, $\gamma_{yz}$ and $\gamma_{zx}$ | the shear strain component |
| $[B]$ | geometric matrix |
| $[D]$ | elasticity matrix |
| $[\delta]$ | nodal displacement matrix |
| $[F]$ | integral nodal load matrix |
| $[K]$ | integral stiffness matrix |

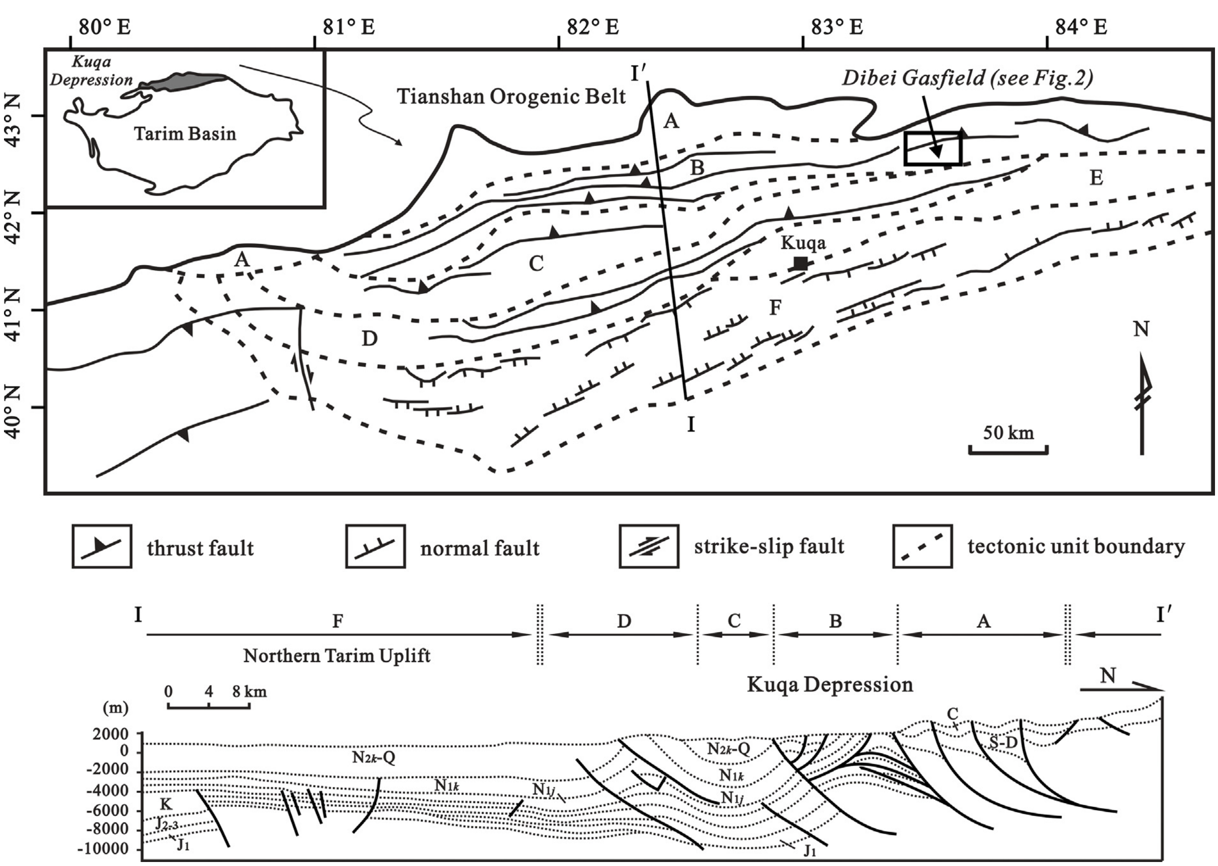


**Fig. 1.** Structural simplified map of the Kuqa Depression within Tarim Basin, China.
Tectonic units: A: Northern monocline tectonic zone; B: Kelasu-Yiqikelike tectonic zone; C: Baicheng sag; D: Qiulitage tectonic zone; E: Yangxia sag; F: Northern Tarim Uplift.
Sedimentary layers: S-D: Silurian to Devonian; C: Carboniferous; $J_1$: Lower Jurassic; $J_{2-3}$: Middle to Upper Jurassic; K: Cretaceous; $N_1j$: Jidike Formation; $N_1k$: Kangcun Formation; $N_2k$: Kuche Formation; Q: Quaternary.